Electric Power Systems Research 203 (2022) 107646

Contents lists available at ScienceDirect

Electric Power Systems Research

journal homepage: www.elsevier.com/locate/epsr

Influence of pulse rise time and duty cycle on distribution of transients along the wind turbine step-up transformer windings

Anurag A. Devadiga [a,*], Shesha H. Jayaram [a]

[a] Electrical and Computer Engineering, University of Waterloo, 200 University Avenue West, Waterloo, ON, N2L 3G1 Canada

ARTICLE INFO

Keywords:
Repetitive transient voltage
Transformers
Frequency response analysis
Transient response analysis
Tap-to-tap voltage

ABSTRACT

A transformer is one of the most important assets in an electric power generation system. Wind turbine step-up transformers have recently seen premature failures due to high-frequency repetitive transients. The high-frequency transients under resonance can severely damage the insulation of the transformer. Thus the paper initially analyses the distribution of transformer frequency response to identify critical resonance frequencies for the two transfer function frequency responses; namely, impedance frequency response and voltage ratio response. Transformer frequency response is compared with transient response to understand the influence of repetitive transient parameters; namely applied voltage amplitude, rise time, and duty cycle, on transient distribution along the transformer winding. Based on three variable experiments, the range of rise time was considered as less than 300 ns and 1000 ns, applied voltage considered was 100 V and 1000 V, and duty cycle considered was 10% and 50%. For the current transformer model, both the experimental and PSCAD simulation results indicated that a duty cycle of 50% and rise time $<$ 300 ns were critically damaging to transformer insulation. The research helps in designing transformer insulation stressed under different transient parameters.

1. Introduction

The operation of vacuum circuit breakers (VCBs) and switching devices produce transient voltages that cause insulation failure of wind turbine transformers, particularly to the first and last transformers in the wind farm chain, as they are the most vulnerable to these transients [1]. These voltage transients have a high rate of rise, high amplitude, and high-frequency components that can overstress the wind turbine transformer leading to premature ageing and transformer insulation failure. The voltage transients, due to prestrike and reignition of the VCB, are amplified based on cable parameters, circuit breaker type, and transformer type present in the wind farm [2, 3]. Liu et al. simulated switching operation of the vacuum circuit breaker in an offshore wind farm and obtained a transient voltage with a rate of rise of 142 kV/μs and an amplitude of 1.3 per unit [4]. Xin et al. obtained transient voltage with a rate of rise of 148 kV/μs and an oscillation frequency of 0.78 kHz at the wind turbine transformer during switching operation of the vacuum circuit breaker [5]. In [6], Zhou et al., show that the increase in the reignition rate of the circuit breaker can increase the rate of rise and amplitude of the voltage transient. Various mitigation techniques like the use of surge arresters were designed to reduce overvoltage at the transformer terminals caused by high-frequency transients, but the arresters are unable to reduce the voltage rate of rise [2]. The arresters can only reduce the amplitude of the transients; whereas, an RC snubber in the wind turbine transformer terminal can reduce both amplitude and rate of rise of the high-frequency transients; cost and installation space need to be considered while considering use of RC snubbers [7–10]. To reduce the rate of rise of the breaker generated transient voltages, Smugala et al. designed a series-connected choke [2]. The authors also used an additional suppressing resistor to reduce the voltage transient level and oscillations. Xin et al. simulated the switching operation of a vacuum circuit breaker for an offshore wind farm to study the voltage transient developed for a 690 V/33 kV wind turbine transformer [11]. A voltage rise of 1.6 p.u. at the transformer for switching operation of VCB's, was obtained and the R-L choke helped reduce the rate of rise of the transient voltages; whereas, the RC filters helped reduce the transformer terminal voltage amplitude to 1.02 p.u [11]. Although the RC snubbers and surge arrestors can be used to mitigate the transient amplitude, rate of rise, and repetitive occurrence, it is difficult to design an RC snubber or an arrestor for a complicated wind turbine topology. Thus, transformer behaviour during high-frequency transient voltage, needs to be studied in order to design the transformer turn-to-turn

* Corresponding author.
E-mail address: aadevadi@uwaterloo.ca (A.A. Devadiga).

https://doi.org/10.1016/j.epsr.2021.107646
Received 27 April 2021; Received in revised form 21 October 2021; Accepted 22 October 2021
Available online 5 November 2021

insulation that can withstand high-frequency transients.

Furthermore, transient voltage created by the switching operation of the circuit breaker can be lower in amplitude but can lead to large internal voltages within the transformer when the frequency of oscillation of the transient matches the frequency characteristics of the transformer [12]. These large voltages can cause permanent damage to the insulation of the transformer. Zhao et al. showed that a transient impulse with a rise time of less than 2 μs can have frequency components with an energy spectrum of about 1 MHz, hence there is a high likelihood for transformer frequency resonance to match the frequency component of the transient [13]. A standard lightning impulse has most of its energy density in the frequency range below a few kHz; whereas transients with steep rise time, front/tail chopped, oscillating components have higher energy in the high-frequency region (1 kHz to 10 MHz) [14]. Resonance frequency oscillation is highest for turn-to-turn as compared to layer-to-layer and section-to-section resonance [15]. The maximum turn-to-turn voltage appears in the end turn of the winding [15]. Soloot et al. [16, 17] studied the internal voltage distribution as a function of frequency, for resonance overvoltages in three transformer designs, namely layer, disc, and pancake windings. Based on the internal resonance frequency response analysis, the authors concluded the disc winding configuration of the wind turbine transformer is more vulnerable to gassing and insulation failures during voltage transients [16]. Also, the authors determined that pancake winding is the least vulnerable design for resonance overvoltage [17].

Khanali et al. [18] studied the effects of an electrostatic shield between LV and HV windings in reducing the transfer of high-frequency transients between the windings by capacitively decoupling them. The authors showed the addition of an electrostatic shield between LV and HV windings reduces the transfer of high-frequency transients at certain frequencies but it also amplifies the transfer of high-frequency transients at other frequencies. Elhaminia et al. studied the influence of disk space, turn insulation thickness, and distance between LV and HV windings on the internal resonance amplification for a wind turbine transformer [19]. The authors suggested the winding resonance can be shifted by increasing the distance between LV and HV winding, while the disk space and turn insulation thickness should be low to reduce the resonance frequency amplification. Sriyono et al. used the sweep frequency response analysis and found that above 200 kHz, there is an increased potential for internal winding resonance amplifications for a 10-kVA layer type transformer [20]. It was shown the voltage level at three-quarters of the winding can be higher than the voltage level at full winding due to internal winding resonance. Even though a considerable amount of research was carried out to study the transformer frequency response to recognize resonance amplification, the literature is unable to demonstrate the difference in various transfer functions to show resonance frequency amplification. The current paper shows the capability of the two transfer function frequency responses; namely, impedance frequency response and voltage ratio response, to show the tap-to-tap voltage difference amplification at resonance frequencies. This paper also correlates the transfer function frequency response with the transient response of the transformer for various parameters of the transient voltage.

With respect to transient voltage parameters, Hassan et al. [21] studied the influence of cable length, rise time, and fall time of the impulse at the peak of transient voltage. It was found the amplitude of the lightning impulse striking the transformer terminal decreases with an increase in impulse rise time, but the fall time does not affect amplitude significantly. Yang et al. analysed the influence of the pulse width and the tail time of the transient impulse voltage on its distribution along the transformer winding [22]. The authors found that a decrease in the transient's pulse width or decrease in the transient's tail time can lead to an increase in the uneven (non-linear) distribution of voltage along the transformer winding. Abdulahovi studied the distribution of the lightning and switching transients along the winding for a single-phase reactor rated at 10 kV and 200 kVA [23]. The impulse applied was the standard lightning impulse of a rise time of 1.2 μs, and step voltage with a rise time ranging from 35 ns to 500 ns. A shorter rise time leads to higher turn-to-turn voltage and its derivative because a shorter rise time can lead to inter-turn resonance, thereby increasing the high voltage at the initial turns of the disc. The basic insulation level is designed based on the standard lightning impulse test; however, as observed from the work of [23] terminals stressed under a shorter rise time, step voltage can lead to turn-to-turn voltages higher than lightning impulse. Ansari et al. used a 12-coil and an 18-coil section transformer simulation models to evaluate the non-uniform voltage distribution along the transformer for fast rise time impulse voltages [24]. The highest voltage stresses were observed at the initial two coils for lightning, switching, and chopped voltage waveforms. The distribution of lightning impulse along each section of a dry-type transformer winding was obtained by Liu et al. [25]. They found the maximum of impulse voltage exceeds the input and is located in sections 3, 4, 5 of the transformer rather than in the first section. Florkowski et al. studied the distribution of rectangular, sinusoidal sweep, chirp signal, and sweep ramp waveforms along the transformer winding and compared it with the lightning impulse distribution [26]. The waveforms were studied to replicate the transient voltage during the operation of the surge arrester and circuit breaker. The overvoltage along 1/3 of the transformer turns due to the application of a rectangular, sinusoidal sweep, and sweep ramp waveforms exceeded the overvoltage caused by the standard lightning impulse voltage. Considerable work was carried out in understanding the distribution of transient voltage along the transformer winding, but the experiments were carried out for a single pulse and not for the repetitive transient voltage. In our preliminary work, the influence of transient rise time, amplitude, and duty cycle on the distribution of transient along the transformer was presented [27]. A duty cycle of 50% and a rise time of 120 ns was found to lead to the highest tap-to-tap stress with voltage distribution. The distribution of the repetitive transient voltage along the transformer winding based on repetitive transients rise time, amplitude, and duty cycle are not considered in the literature in detail even though it is an important aspect to designing a transformer's inter-turn insulation.

The transformer internal resonance frequency characteristics have been studied in the past but the correlation between the internal frequency response and transient response along the winding is not completely understood. Hence, it is important to identify the internal resonance frequency to match the transient voltage amplification. The paper presents the methodology of transient and frequency response measurements, and internal frequency response characteristics for two model transformers aged under different waveforms. The transient distribution of the transformer as a function of repetitive transient voltage parameters (amplitude, rise time, and duty cycle) is studied for obtaining the maximum tap-to-tap voltage transient for different cases of transient parameters. Finally, PSCAD simulation of the transformer equivalent circuit is carried out to study the influence of the transient voltage parameters on its distribution along the transformer winding.

2. Methodology and calculations

2.1. Frequency response analysis

The frequency response of two transformers viz., Transformer 1, T1, and Transformer 2, T2 are presented. Transformer 1 was previously aged under sinusoidal voltage and Transformer 2 was previously aged under repetitive high-frequency fast rise time pulses [28]. The transformers T1 and T2 are 115 V / 6.6 kV layered type transformers designed similar to wind turbine step-up transformers. The detailed information about transformers T1 and T2 are provided in [27, 28]. Two types of frequency response measurements are compared; namely, impedance frequency response and voltage ratio frequency response. The schematic diagram of an experimental set-up for the measurement of impedance frequency response is shown in Fig. 1. The source is a sinusoidal voltage of 10

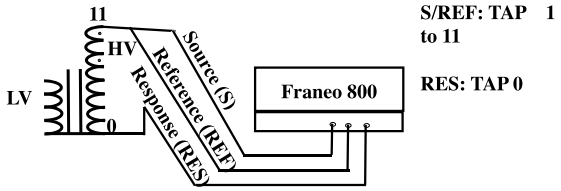

Fig. 1. A schematic diagram of an experimental set-up for the measurement of impedance frequency response.

Vpeak-to-peak with frequency varying from 20 Hz to 2 MHz. The reference voltage, V_{REF} is measured across the source, and the source is moved from tap 1 to 11 independently. The response voltage, V_{RES} is always measured at tap 0. The impedance is calculated by the following formula: 50 $(V_{REF} - V_{RES})/V_{RES}$ and obtained for frequencies from 20 Hz to 2 MHz. The schematic diagram of an experimental set-up for the measurement of voltage ratio response is shown in Fig. 2. The source and the reference are fixed at tap 11 whereas the response is measured from tap 1 to tap 10 individually. The voltage ratio as a function of frequency is obtained by the following formula: V_{RES}/V_{REF}.

2.2. Transient response analysis

The schematic diagram of an experimental set-up for the measurement of transient response is shown in Fig. 3. A repetitive transient voltage is applied at tap 11 and the input probe measures the tap 11 voltage. The output probe measures the response starting from tap 10 to tap 1 individually. The probe used is Tektronix P6015A and the oscilloscope is Rohde & Schwarz, RTO 1024 with a sampling frequency of 10 Gsa/s and bandwidth of 2 GHz. The values for the parameters of the repetitive transient are shown as four cases in Table 1. The parameters varied are voltage amplitude, duty cycle, and rise time. The frequency of the transient voltage is fixed at 1 kHz. This paper uses repetitive high-frequency transient voltage generated by the switching operation of the vacuum circuit breakers in a wind farm chain. In addition, power electronic converters add to the transients but the experimental work presented here considers fast transients generated by the circuit breaker operation.

The pulse parameters, rise time, pulse repetition frequency, and duty cycle used are selected based on the previously published simulation studies by Devgan [3]. The simulation study by Devgan showed that the switching operation of the vacuum circuit breaker generated repetitive transient voltage of rate of rise from 1.1 kV/μs to 10 kV/ μs, and repetition frequency ranging from 450 Hz up to 22 kHz. Accordingly, the applied voltage (100 V to 1000 V) and rise time (300 ns to 1000 ns) were selected based on the rate of rise of the transient voltage obtained in [3]. The duty cycle of 10% and 50% were selected to evaluate the influence of the duration of the transient on its distribution along the transformer winding.

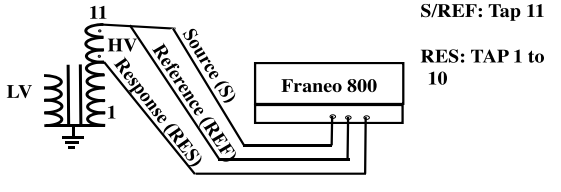

Fig. 2. A schematic diagram of an experimental set-up for the measurement of voltage ratio frequency response.

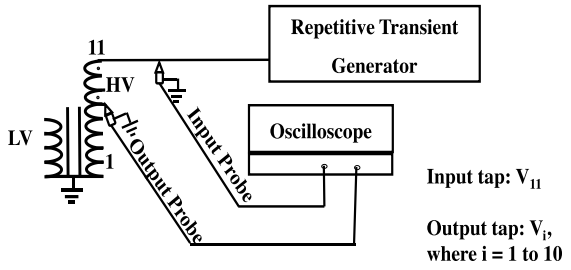

Fig. 3. A schematic diagram of an experimental set-up for the measurement of transient response.

Table 1
Parameters of the repetitive transient.

Cases	Voltage(V)	Duty(%)	Rise time(ns)
Case 1	100	10	100 - 300
Case 2	100	50	100 - 300
Case 3	1000	10	100 - 300
Case 4	100	10	900 - 1100

2.3. PSCAD simulation

The PSCAD simulation of the transformer equivalent circuit is carried out to understand the influence of the transient parameters on the distribution of transients along the transformer taps. The transformer PSCAD equivalent circuit for the final tap, tap 11 is shown in Fig. 4. The tap voltages from tap 1 to tap 11 are simulated and measured similar to experiments on Transformer 1 and Transformer 2. Each tap is divided into four sections and the parameter value of elements of each section is shown in Table 2. The parameters of the elements of each section are obtained from the dimensions of transformers T1, and T2. The winding self-inductance, stray capacitance to tank, tap to tap capacitance, and winding section capacitance are obtained from the geometric calculations derived from the transformer design parameter. The insulation resistance is assumed as a high value in the range of MΩ.

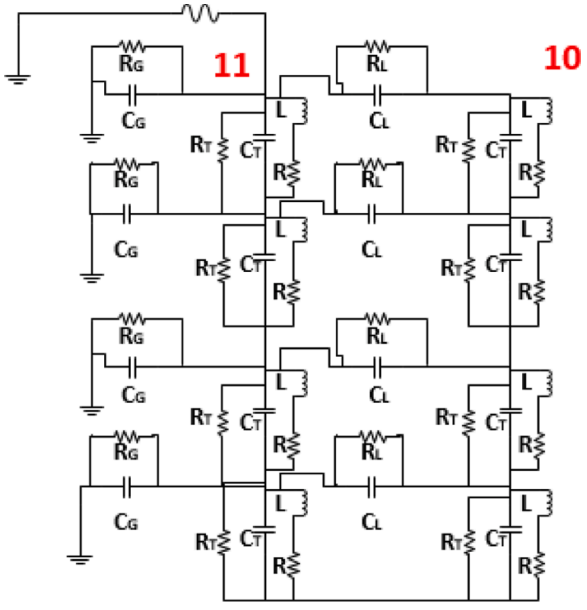

Fig. 4. PSCAD transformer equivalent circuit for tap 11 of the transformer containing 11 taps, similar to the model transformers used in this study.

Table 2
PSCAD transformer equivalent circuit parameter per section of a tap.

Element-Description	Value
L: Winding self-inductance	2.1131 mH
R: Winding resistance	4.5 Ω
C_G: Stray capacitance to tank	0.0597 nF
C_L: Tap to tap capacitance	64.345 nF
C_T: Winding section capacitance	0.7912 pF
R_T, R_G: Dielectric resistance	3 MΩ

3. Results and discussion

3.1. Frequency response analysis

The transformer impedance response as a function of frequency along the taps for Transformer 1 and Transformer 2 is shown in Fig. 5 and Fig. 6 respectively. The impedance response for both transformers is similar. The impedance response curve increases with the increase in tap number at frequencies below 200 Hz, the response is mainly governed by magnetizing inductance. Also, the resonance frequency increases with an increase in tap number which is caused due to cancelling of inductive reactance by series capacitance. There are two resonance frequencies, one between 100 Hz and 1000 Hz, and another around 10,000 Hz. Both frequency regions are critical in terms of resonance match with transient voltage. Fig. 7 and Fig. 8 show the tap-to-tap impedance difference response for Transformers 1 and 2 respectively. The tap-to-tap impedance difference response is obtained by subtracting the previously obtained impedance response for adjacent taps. The response is similar for both Transformers 1 and 2. Similar to the impedance response, the tap-to-tap impedance difference response has two resonance regions, one between 100 Hz and 1000 Hz and the second one around 10,000 Hz. Between 100 Hz and 1000 Hz, the impedance difference response resonance frequency increases with an increase in tap number. But around 10 kHz, it is seen that resonance frequency and amplitude for impedance difference response are highest for tap 1–2 and tap 3–4. Generally, the transient response is highest in the line end that is between tap 9–10 but based on the impedance difference frequency response if the transient signal has a dominant component around 10 kHz then the tap-to-tap resonance can lead to very high voltage transients at the initial taps. The impedance frequency response consideration is therefore critical in designing transformer insulation.

Fig. 9 and Fig. 10 show the transformer voltage ratio response as a function of frequency along the taps for Transformers 1 and 2 respectively. In the frequency region below 10 kHz, the frequency response increases with an increase in tap number as the response is governed by transformer turns ratio and series capacitance. The overall response has no resonance points between 10 kHz and 300 kHz. Fig. 11 and Fig. 12 show tap-to-tap voltage ratio difference response for Transformer 1 and Transformer 2 respectively. Unlike impedance difference response, voltage ratio difference response shows the highest difference amplitude at tap 9–10 (line end taps) and the voltage ratio difference decreases with a decrease in tap number.

The voltage ratio difference response is unable to show the highest difference between tap 1–2. Comparing the results for voltage difference magnitude (dB) [27] and the impedance difference response, it can be seen that both responses show the highest difference between tap 1–2

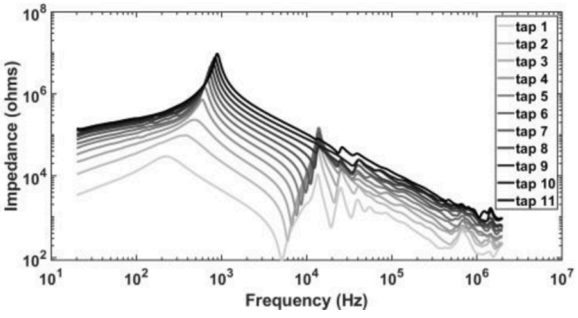

Fig. 5. Transformer impedance response as a function of frequency along the taps in Transformer 1.

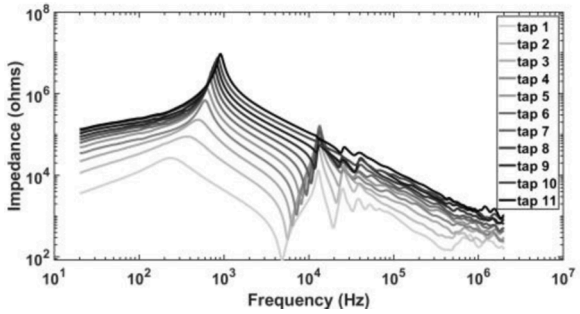

Fig. 6. Transformer impedance response as a function of frequency along the taps in Transformer 2.

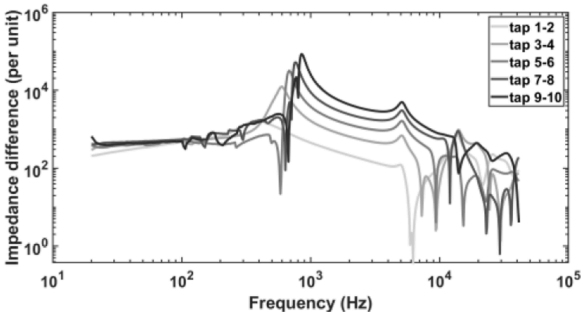

Fig. 7. Tap-to-tap impedance difference response for Transformer 1.

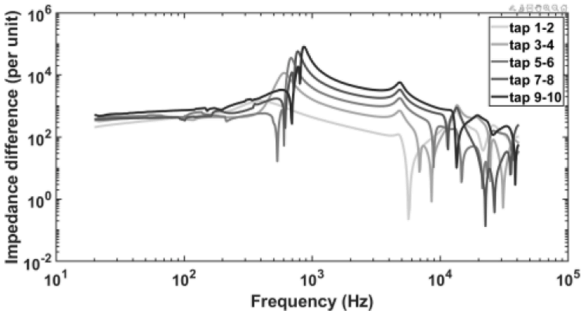

Fig. 8. Tap-to-tap impedance difference response for Transformer 2.

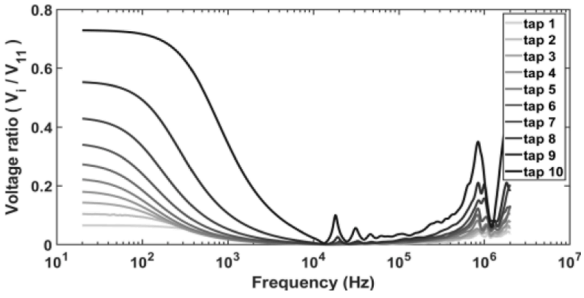

Fig. 9. Transformer voltage ratio response as a function of frequency along the taps in Transformer 1.

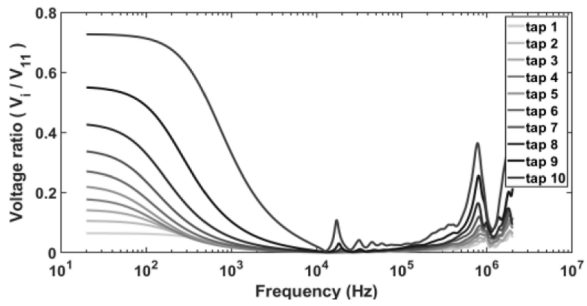

Fig. 10. Transformer voltage ratio response as a function of frequency along the taps in Transformer 2.

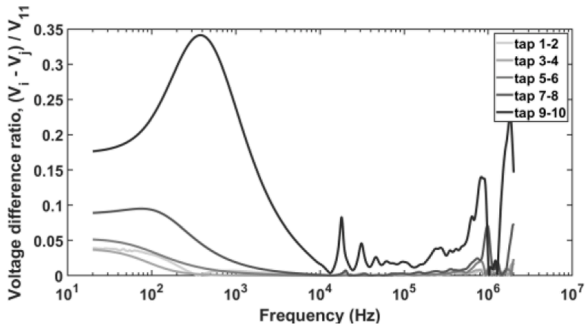

Fig. 11. Tap-to-tap voltage ratio difference response for Transformer 1.

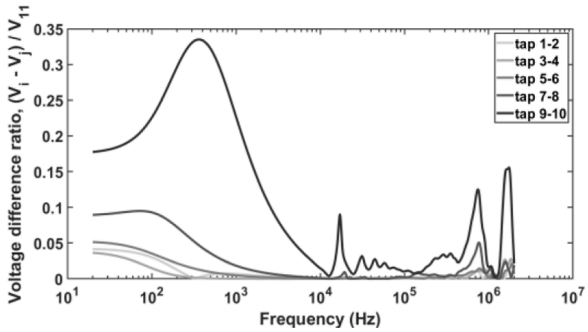

Fig. 12. Tap-to-tap voltage ratio difference response for Transformer 2.

around 10 kHz for both transformers. Voltage difference magnitude (dB) as reported in [27] also shows distinction in the response between Transformer 1 and Transformer 2; whereas, the impedance difference response is unable to show this distinction between the two transformers. Also, different tap-to-tap voltage ratios are not the same at 20 Hz because of the difference in tap-to-tap winding resistance, when moved from tap 1–2 to tap 9–10. The tap-to-tap winding resistance varied from 20 Ω in tap 1–2, to 30 Ω in tap 9–10.

3.2. Transient response analysis

Fig. 13 shows the transient response voltage in p.u. for Transformer 1 for case 3 of the input voltage, with the amplitude of 1000 V, duty cycle of 10%, and rise time of 290 ns respectively. It can be seen from the figure that transient response amplitude increases as we move from core end taps to high voltage terminal taps, and rise time decreases as we move from core end taps to high voltage terminal taps. The transient response is non-uniform along the taps. Tables 3 and 4 show rise time along taps (taps 10, 6, 3) respectively for Transformer 1 and Transformer 2 for the four cases of transient voltages. It is seen from the results that for tap 10 and tap 6, the lower rise time (faster transient) is obtained for

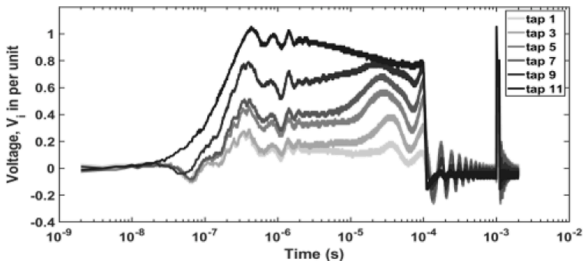

Fig. 13. Repetitive transient response voltage in p.u. along Transformer T1 for an input voltage of case 3: amplitude = 1000 V, duty cycle = 10%, rise time = 290 ns.

Table 3
Rise time along the taps for various cases of transient parameters for Transformer 1.

Cases	Tap 10(ns)	Tap 6(ns)	Tap 3(ns)
Case 1	260	28,700	46,500
Case 2	701	23,700	28,700
Case 3	232	19,100	42,100
Case 4	10,900	26,800	35,900

Table 4
Rise time along the taps for various cases of transient parameters for Transformer 2.

Cases	Tap 10(ns)	Tap 6(ns)	Tap 3(ns)
Case 1	280	28,600	53,700
Case 2	518	19,200	31,700
Case 3	227	18,400	20,600
Case 4	9660	21,200	38,300

case 3 of the input voltage with an amplitude of 1000 V, duty cycle of 10%, and rise time of 290 ns. The rise time increases with a decrease in tap number because as the transient travels along the winding, the surge is attenuated and dispersed. The rise time values of Transformer 2 are lower than Transformer 1 for taps 10 and 6. Transformer 2 is aged under repetitive transients, whereas, Transformer 1 is aged under sinusoidal voltage. For tap 3, the lowest rise time for Transformer 1 and Transformer 2 is with case 2 and case 3 of transient voltage respectively. The tap-to-tap voltage difference in per unit for various cases of transient voltages for Transformer 1 and Transformer 2 are shown in Fig. 14 and Fig. 15. From both the figures it can be seen the tap-to-tap voltage difference is highest for end taps. Amongst the four cases, case 2 with an amplitude of 100 V, a duty cycle of 50%, and a rise time of 290 ns has the highest tap-to-tap voltage difference.

Fig. 16 and Fig. 17 show the tap-to-tap voltage difference in per unit for fast fourier transform (FFT) of transient voltage cases for Transformer 1 and Transformer 2. These figures show the tap-to-tap voltage difference for the transformers at a frequency of 10 kHz. This frequency

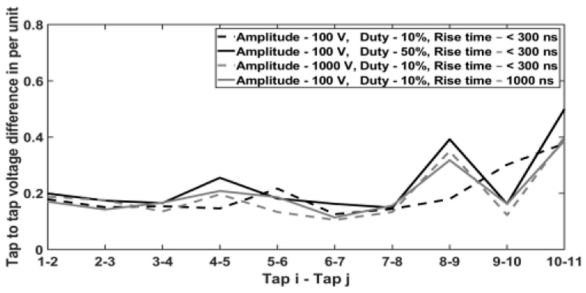

Fig. 14. Tap-to-tap transient voltage difference in per unit along Transformer 1 for various cases of transient voltage.

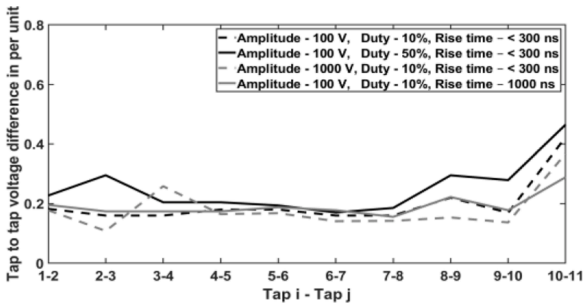

Fig. 15. Tap-to-tap transient voltage difference in per unit along Transformer 2 for various cases of transient voltage.

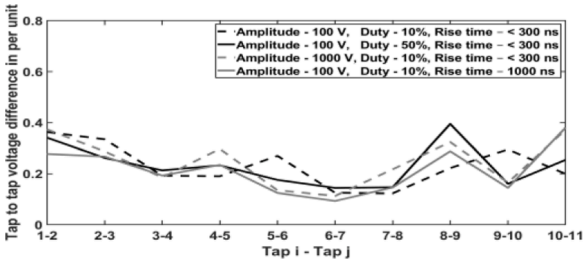

Fig. 16. Tap-to-tap transient voltage difference in per unit along Transformer 1 for various cases of transient voltage (FFT).

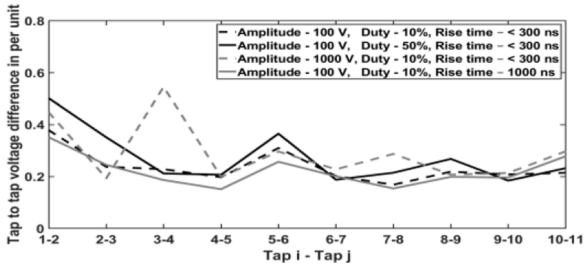

Fig. 17. Tap-to-tap transient voltage difference in per unit along Transformer 2 for various cases of transient voltage (FFT).

component is chosen from impedance difference frequency response characteristics (Fig. 7 and Fig. 8). The frequency content of the fast transient are from 1 kHz to 1 MHz. In the current study, the transformer's critical resonance frequency based on its design is 10 kHz and when the frequency of the repetitive transient matches the resonance frequency of the transformer, it would lead to significantly large voltages, and might result in failure of the transformer insulation. It is clear from the figure that the highest tap-to-tap voltage is seen in the initial taps of the winding where the second resonance was observed. In Fig. 17, resonance amplification at tap 3–4 is seen when voltage level of 1000 V, with the rise time of 290 ns is applied to the transformer 2. The resonance amplification at tap 3–4 is not observed when a voltage level of 100 V was applied. These observed differences can be related to the transient voltage wave travelling along the network of R, L and C between taps. The model transformers used in this study consist of 748 turns between two taps. The conductors, enamel coating, oil and paper insulation, together, form a network of inductances, capacitances and resistances. Thus, the transient voltage of amplitude, 1000 V and a rise time of 290 ns, resulting in steeper dV/dt would have led to resonance amplification at tap 3–4 in Fig. 17 as compared to the voltage waveform with an amplitude of 100 V. The paper shows that a difference in rate of rise can lead to tap-to-tap resonance amplification at the initial taps of the transformer winding based on the frequency characteristics of the overall RLC network between taps. Comparing the four cases of transient voltage (FFT), it is difficult to say the transient voltage case has the highest tap-to-tap voltage difference.

Comparing the time domain results (Fig. 14 and Fig. 15) to the frequency domain results (Fig. 16 and Fig. 17), it can be seen that time domain results show the highest tap to tap voltage difference in the end taps, tap 10–11; whereas, the frequency domain results show highest tap to tap voltage difference in the initial taps, tap 1–2. Therefore, there are chances of amplification of transient voltages due to resonance at the initial taps if the transformer's critical frequency matches the frequency of the repetitive transient voltage generated by the switching operation of the circuit breaker.

3.3. PSCAD simulation

Fig. 18 shows the repetitive transient response for the PSCAD simulation of transformer equivalent circuit for transformer input voltage transient of amplitude = 100 V, duty cycle = 10%, rise time = 200 ns. Comparing the simulation to the experimental response in Fig. 13, it can be seen the simulation response has a large peak and oscillation. This is because the simulation response is not a replica of the actual transformers in terms of frequency response.

Fig. 19 shows the rate of rise along the taps in per unit for different transient cases for PSCAD transformer response simulation. The rate of rise is highest for case 2 with an input voltage amplitude of 100 V, duty cycle of 50%, and rise time of 200 ns. Also, the rate of rise increases with an increase in tap number except for case 2. The rate of rise in per unit for case 1 and case 3 of input transient voltage coincide with each other, so in the present simulation study, the amplitude of the transient voltage is not a significant factor for the rate of rise. Case 4 has the lowest rate of rise for input transient voltage rise time of 1000 ns. The tap-to-tap voltage difference in per unit for PSCAD simulation of transformer response for different transient voltage cases is shown in Fig. 20. It can be seen from the figure the highest tap-to-tap voltage difference occurs for case 2 with an input voltage amplitude of 100 V, duty cycle of 50%, and a rise time of 200 ns which matches the experimental transformer tap-to-tap voltage difference in Fig. 14 and Fig. 15. The tap-to-tap voltage difference for cases 1, 3, and 4 are similar. Case 2 has the highest tap-to-tap voltage difference because the rise time of 200 ns and the duty cycle of 50% has the highest voltage energy spectrum. The transient voltage amplitude did not influence the tap-to-tap voltage difference significantly in Fig. 20 because the PSCAD simulation study is based on the design parameters of the transformer that includes just the high frequency characteristics of the transformer modelled using simple lumped elements. The experimental results in Figs. 14 to 17 include all the materials properties and coupling effects of the transformer, thus there is a difference in transformer behaviour for tap-to-tap transient voltage difference as a function of applied transient voltages. For the current model transformer, the experimental results and the PSCAD simulation results match well in terms of overall trend, and thus the PSCAD simulation can be extended to analyse the distribution of transients along windings of other transformer models in a wind farm chain.

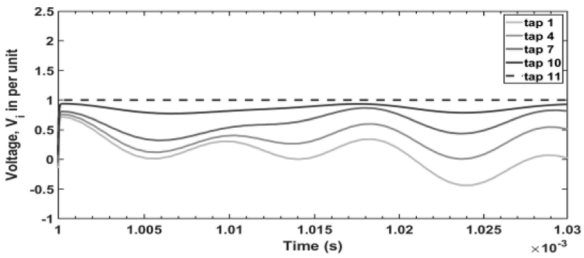

Fig. 18. Repetitive transient transformer response for PSCAD simulation for an input voltage of case 1: amplitude = 100 V, duty cycle = 10%, rise time = 200 ns.

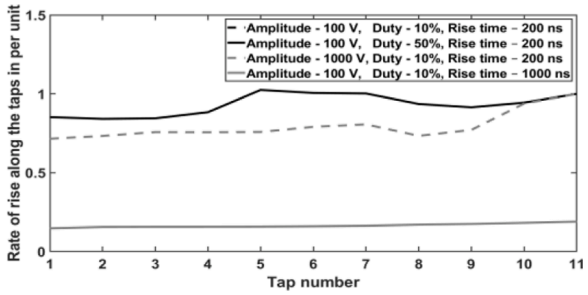

Fig. 19. Rate of rise along taps in per unit for PSCAD simulation of transformer response for different cases of transient input voltage.

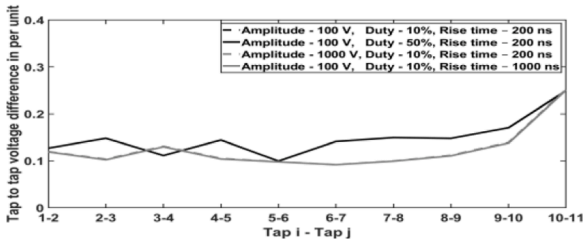

Fig. 20. Tap-to-tap voltage difference in per unit for PSCAD simulation of transformer response for different cases of transient input voltage.

4. Conclusion

The operation of switching devices combined with the frequency characteristics of the transformer can lead to high-frequency high amplitude transients on wind turbine step-up transformer insulation. This paper focused on experimentally investigating the effects of pulse parameters on the distribution of high-frequency transient voltage along the wind turbine step-up transformers. Both the frequency and transient responses are used.

Comparing impedance and voltage ratio frequency responses, the impedance frequency response gives an identifiable signature for tap-to-tap resonance at the initial tap region (tap 1–2) which is critical in designing the transformer insulation for high-frequency transients. Based on the variation of transient response parameters it is concluded that rise time less than 300 ns and the duty cycle of 50% can lead to critical tap-to-tap voltage levels. The FFT of transient response confirms the amplification of transient voltage at tap 1–2, which is also captured by impedance frequency difference response but undetected by voltage ratio difference response. The voltage difference magnitude (dB) predicted the difference in ageing between Transformer 1 and Transformer 2.

A simplified PSCAD simulation model based on the design parameters of the transformer that include just its high frequency characteristics is presented. Although the overall trends observed match, there exists differences between the measured and simulated results. This can be explained by the fact that the experimental results reflect the measured data, which include the actual material properties and coupling effects of the transformer.

CRediT authorship contribution statement

Anurag A. Devadiga: Methodology, Software, Investigation, Formal analysis, Writing – original draft, Writing – review & editing, Project administration. **Shesha H. Jayaram:** Conceptualization, Methodology, Validation, Formal analysis, Resources, Writing – review & editing, Supervision, Project administration, Funding acquisition.

Declaration of Competing Interest

The authors declare that they have no known competing financial interests or personal relationships that could have appeared to influence the work reported in this paper.

Acknowledgments

The authors would like to thank the Natural Sciences and Engineering Research Council of Canada (NSERC) for funding the research work.

References

[1] IEC/IEEE 60076-16 Edition 2.0, Power transformers - Part 16: transformers for wind turbine applications, pp.1–26, 28 Sept. 2018. doi: 10.1109/IEEESTD.2018.8476640.
[2] D. Smugala, W. Piasecki, M. Ostrogorska, M. Florkowski, M. Fulczyk, O. Granhaug, Wind turbine transformers protection method against high-frequency transients, IEEE Trans. Power Delivery 30 (2) (2015) 853–860, https://doi.org/10.1109/TPWRD.2014.2343261. April.
[3] M. Devgan, Investigation of High Frequency Switching Transients On Wind Turbine Step Up Transformers, MASc. Thesis, University of Waterloo, Canada, 2015.
[4] G. Liu, Y. Guo, Y. Xin, L. You, X. Jiang, M. Zheng, W. Tang, Analysis of switching transients during energization in large offshore wind farms, Energies 11 (470) (2018) 1–13, https://doi.org/10.3390/en11020470.
[5] Y.L. Xin, W.H. Tang, J.J. Zhou, Y.H. Yang, G. Liu, Sensitivity analysis of reignition overvoltage for vacuum circuit breaker in offshore wind farm using experiment-based modeling, Electr. Power Syst. Res. 172 (2019) 86–95, https://doi.org/10.1016/j.epsr.2019.02.008. ISSN 0378-7796.
[6] Q. Zhou, Y. Cheng, X. Bian, F. Liu, Y. Zhao, Analysis of restrike overvoltage of circuit breakers in offshore wind farms, IEEE Trans. Appl. Supercond. 26 (7) (2016) 1–5, https://doi.org/10.1109/TASC.2016.2594830. Oct.Art no. 0607905.
[7] J. Zhou, W. Tang, Y. Xin, Q. Wu, Investigation on switching overvoltage in an offshore wind farm and its mitigation methods based on laboratory experiments. 2018 IEEE PES Asia-Pacific Power and Energy Engineering Conference (APPEEC), Kota Kinabalu, 2018, pp. 189–193, https://doi.org/10.1109/APPEEC.2018.8566662.
[8] J. Zhou, Y. Xin, W. Tang, G. Liu, Q. Wu, Impact factor identification for switching overvoltage in an offshore wind farm by analyzing multiple ignition transients, IEEE Access 7 (2019) 64651–64662, https://doi.org/10.1109/ACCESS.2019.2916952.
[9] S. Ghasemi, M. Allahbakhshi, B. Behdani, M. Tajdinian, M. Popov, Probabilistic analysis of switching transients due to vacuum circuit breaker operation on wind turbine step-up transformers, Electr. Power Syst. Res. 182 (106204) (2020) 1–9, https://doi.org/10.1016/j.epsr.2020.106204.
[10] Y. Guo, X. Jiang, Y. Chen, M. Zheng, G. Liu, X. Li, W. Tang, Reignition overvoltages induced by vacuum circuit breakers and its suppression in offshore wind farms, Int. J. Electr. Power Energy Syst. 122 (106227) (2020) 1–7, https://doi.org/10.1016/j.ijepes.2020.106227.
[11] Y.L. Xin, W.H. Tang, L. Luan, G.Y. Chen, H. Wu, Overvoltage protection on high-frequency switching transients in large offshore wind farms. 2016 IEEE Power and Energy Society General Meeting (PESGM), Boston, MA, 2016, https://doi.org/10.1109/PESGM.2016.7741642.
[12] IEEE Std C57.142-2010, IEEE guide to describe the occurrence and mitigation of switching transients induced by transformers, switching device, and system interaction, pp.1–56, 27 April 2011. doi: 10.1109/IEEESTD.2011.5759579.
[13] X. Zhao, C. Yao, Z. Zhao, A. Abu-Siada, Performance evaluation of online transformer internal fault detection based on transient overvoltage signals, IEEE Trans. Dielectr. Electr. Insul. 24 (6) (2017) 3906–3915, https://doi.org/10.1109/TDEI.2017.006772. Dec.
[14] M. Kuniewski, P. Zydron, Analysis of the applicability of various excitation signals for FRA diagnostics of transformers. 2018 IEEE 2nd International Conference On Dielectrics (ICD), Budapest, 2018, pp. 1–4, https://doi.org/10.1109/ICD.2018.8514677.
[15] IEEE Std C57.12.58-2017, IEEE guide for conducting a transient voltage analysis of a dry-type transformer coil, pp.1–30, 13 Nov. 2017. doi: 10.1109/IEEESTD.2017.8126273.
[16] A.H. Soloot, H.K. Høidalen, B. Gustavsen, Influence of the winding design of wind turbine transformers for resonant overvoltage vulnerability, IEEE Trans. Dielectr. Electr. Insul. 22 (2) (2015) 1250–1257, https://doi.org/10.1109/TDEI.2015.7076828. April.
[17] A.H. Soloot, H.K. Høidalen, B. Gustavsen, Modeling of wind turbine transformers for the analysis of resonant overvoltages, Electr. Power Syst. Res. 115 (2014) 26–34, https://doi.org/10.1016/j.epsr.2014.03.004.
[18] M. Khanali, S.H. Jayaram, Effectiveness of electrostatic shielding in suppressing the impact of fast transients on transformer insulation. 2015 IEEE Conference on Electrical Insulation and Dielectric Phenomena (CEIDP), Ann Arbor, MI, 2015, pp. 652–655, https://doi.org/10.1109/CEIDP.2015.7352146.

[19] P. Elhaminia, M. Vakilian, M. Lehtonen, Wind turbine transformer improved design method entailing resonance blocking, IET Electr. Power Appl. 12 (9) (2018) 1337–1343, https://doi.org/10.1049/iet-epa.2018.5165.
[20] S. Sriyono, U. Khayam, S. Suwarno, SFRA characteristics of power transformer internal winding considering the resonant effect, 8th International Conference on Condition Monitoring and Diagnosis (CMD), 2020, pp. 302–305. doi: 10.1109/CMD48350.2020.9287194.
[21] E.O. Hassan, E.A. Badran, F.M.H. Youssef, Effect of lightning impulses on the resonance stresses in the high voltage power transformers. 2017 Nineteenth International Middle East Power Systems Conference (MEPCON), Cairo, 2017, pp. 496–502, https://doi.org/10.1109/MEPCON.2017.8301226.
[22] Q. Yang, Y. Chen, W. Sima, H. Zhao, Measurement and analysis of transient overvoltage distribution in transformer windings based on reduced-scale model, Electr. Power Syst. Res. 140 (2016) 70–77, https://doi.org/10.1016/j.epsr.2016.06.039.
[23] T. Abdulahovic, Analysis of High-Frequency Electrical Transients in Offshore Wind Parks, Ph. D. Thesis, Chalmers University of Technology, Sweden, 2011.
[24] M.Z.A. Ansari, J. Akhtar, Time domain analysis of a 12 coil section and 18 coil section transformer model winding subjected to a variety of surge voltages. 2015 International Conference on Power and Advanced Control Engineering (ICPACE), Bangalore, 2015, pp. 405–408, https://doi.org/10.1109/ICPACE.2015.7274981.
[25] L. Liu, S. Wang, Y. Pan, Z. Peng, Analysis of lightening impulse response of cast resin dry-type transformer. 2018 12th International Conference On the Properties and Applications of Dielectric Materials (ICPADM), Xi'an, 2018, pp. 876–879, https://doi.org/10.1109/ICPADM.2018.8401168.
[26] M. Florkowski, J. Furgał, M. Kuniewski, P. Pająk, Comparison of transformer winding responses to standard lightning impulses and operational overvoltages, IEEE Trans. Dielectr. Electr. Insul. 25 (3) (2018) 965–974, https://doi.org/10.1109/TDEI.2018.007001. June.
[27] A.A. Devadiga, S.H. Jayaram, The influence of repetitive transient parameters on the distribution of transients along the transformer winding. 2020 IEEE Electrical Insulation Conference (EIC), Knoxville, TN, USA, 2020, pp. 309–312, https://doi.org/10.1109/EIC47619.2020.9158685.
[28] M. Khanali, S. Jayaram, Dielectric frequency response of transformer insulation system under high-dV/dt stresses. 2015 IEEE 11th International Conference On the Properties and Applications of Dielectric Materials (ICPADM), NSW, Sydney, 2015, pp. 408–411, https://doi.org/10.1109/ICPADM.2015.7295295.